

Methanol synthesis in a high-pressure membrane reactor with liquid sweep

Zhongtang Li and Theodore T. Tsotsis*

Mork Family Department of Chemical Engineering and Materials Science, University of Southern California, University Park, Los Angeles, CA 90089-1211, United States

Keywords: methanol synthesis, membrane reactor, liquid sweep, catalyst, inorganic membrane, membrane surface modification

*Corresponding Author

Email address: tsotsis@usc.edu

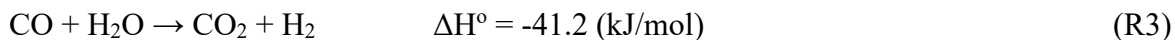
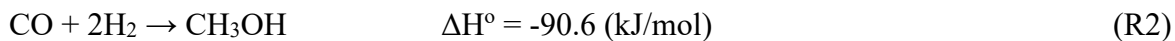
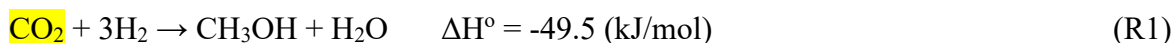
ABSTRACT

Membrane reactors (MR) are known for their ability to improve the selectivity and yield of chemical reactions. In this paper, a novel high-pressure MR employing a liquid sweep was applied to the methanol synthesis (MeS) reaction, aiming to increase the per single-pass conversion. For carrying-out the reaction, an asymmetric ceramic membrane was modified with a silylating agent in order to render its pore surface hydrophobic. A commercial MeS catalyst was used for the reaction, loaded in the MR shell-side, while the tube-side was swept with a high boiling point organic solvent with high solubility towards methanol. The membrane reactor was studied under a variety of experimental conditions (different pressures, temperatures, space times, and liquid sweep flow rates) and showed improved carbon conversion when compared to the conventional packed-bed reactor operating under the same conditions.

1. Introduction

A consequence of a growing world population along with continued industrialization, is the increased global demand for energy. Today, fossil fuel resources such as natural gas (NG), crude oil, and coal dominate the world's energy supply. These traditional energy resources are, however, limited in size, and the fast-growing world population and the booming economies of developing countries such as China and India further intensify concerns about their future availability. Another concern with fossil fuels is the carbon dioxide (CO₂) emissions produced during their combustion for power generation. CO₂ is thought today to be a key contributor to global warming, and its emissions may have to be reduced considerably to avoid potential catastrophic consequences in the future. One way to decrease the world's reliance on fossil fuels and to decrease the potential environmental impacts is the use of renewable energy sources, like solar and geothermal energy, biomass, wind and ocean wave power [1, 2]. Another way is to convert the CO₂, from power generation with fossil fuels into chemicals and fuels (this is known as carbon capture and utilization (CCU)).

Methanol (MeOH) is among the most important/versatile industrial materials with numerous applications such as a feedstock for producing various chemicals (e.g., C₂-C₄ olefins and aromatics [3-5]), fuels and fuel additives like DME, MTBE and DMC [6-8]), and as hydrogen carrier in energy storage. Converting CO₂ into MeOH is a promising CCU route and has attracted recent attention. Methanol can be synthesized via several methods including the direct oxidation of methane [9], but the common approach today is catalytically from syngas (a mixture of CO, CO₂ and H₂) produced from either coal (via gasification) or NG (via steam reforming or partial oxidation). The reactions reported as taking place during methanol synthesis (MeS) are shown below.



Though we list all three reactions here, due to the fact that different research groups still hold different opinion on the carbon source for methanol during MeS, it should be noted that only two out of these three reactions are linearly independent. In our fitting of our kinetic data, as discussed later, we only use reactions R1 and R3. The overall MeS reaction is exothermic and associated with a mole decrease, meaning that high-pressure and low-temperature operating conditions are favored thermodynamically.

The commercial so-called low-pressure Cu-ZnO-Al₂O₃ MeS catalyst commonly employed today (including in this study) is highly selective (selectivity, typically, >99 %), with DME being the main by-product [9]. There are today several commercial MeS processes (e.g., Lurgi [2], Johnson Matthey/Davy Process Technology [2], and Haldor-Topsoe [10]), and though they differ in their technical features, they all try to overcome two key challenges that MeS faces under these relatively low-pressure conditions: low per-pass conversions that dictate recycle of the unreacted syngas [2], and the need to efficiently remove the reaction heat. These challenges have also motivated the continued development of novel MeS processes [11-17], but none has reached commercial maturity. The low per-pass conversion is particularly problematic for MeOH production from renewable biomass, and from the so-called stranded gas from oil extraction operations. These are small-scale, distributed-type applications for which the large-scale commercial processes do not provide an efficient solution. For example, the syngas produced from biomass gasification will likely have a large N₂ content, since the use of oxygen-blown gasifiers is not economic for such an application because of the costs involved in the installation of an air separation unit (ASU). For these applications, increasing the per-pass conversion (to ~85%) is key to commercial adaptation, which requires being able to substantially overcome the thermodynamic limitations of the MeS reaction. Reactive separation processes, including membrane reactors (MR), are potentially of interest in this area.

MR have, indeed, been studied previously for MeS (and also for the related Fischer-Tropsch (FT) reaction) to overcome low conversion and thermal management hurdles [18-27]. Galucci et al. [20], e.g., studied a packed-bed MR (PBMR) for MeS using a commercial Cu-Zn catalyst and a zeolite-A membrane. Under the same level of conversion, the PBMR gave higher selectivity than the conventional PBR due to the selective removal of H₂O and CH₃OH via the

membrane. Earlier, Barbieri et al. [21] predicted such behavior via simulations. Struis et al. [23] carried-out an experimental study of MeS in a MR employing a Nafion® membrane which is permselective towards methanol and water, with the syngas flowing in the membrane tube-side (loaded with Sud-Chemie AG Cu/Zn catalyst), and with sweep gas (Argon) flowing counter-currently in the shell-side. They examined membranes with different counter-ions (e.g., Li⁺, H⁺ and K⁺) at temperatures up to 200 °C and demonstrated improvements in reactor performance by increasing the pressure, and by optimizing the membrane structure and the module configuration. A model was also developed for the validation of the experimental results [24]. Chen and Yuan [25] performed a similar study using a silicone rubber composite membrane on alumina support and observed higher conversion in the PBMR over the traditional reactors. The experimental conversions were <10%, however, and there is concern about the long-term stability of such membranes under the high pressure/temperature MeS conditions. A modeling study of a MR for MeS that uses a water-permselective silica membrane for the in situ water removal (via a permeate-side sweep) to achieve a higher rate of methanol production was carried out by Farsi and Jahanmiri [28]. A modest enhancement in conversion over equilibrium (~4 %) was predicted, but a potential added benefit of removing the water was noted, which is enhanced catalyst lifetime, since water is also thought to promote catalyst deactivation via sintering.

Distributor-type MRs have also been studied for the FT process and for alcohol synthesis [22, 26, 27, 29-35], including MeS. Rahimpour and Ghader [22], e.g., simulated a Pd-membrane based distributor-type MR for MeS in which the catalyst is placed in the membrane tube-side where the syngas is fed to and the reaction takes place; additional H₂ is fed into the membrane shell-side and permeates through the membrane to reach the reactor side, the idea here being to adjust “on the fly” the H₂ concentration in the tube-side for optimal performance. The concept has yet to be validated experimentally, though. Rahimpour and coworkers also modeled several dual-reactor systems [36-40]. For example, they studied a distributor-type MR [41-43] that coupled MeS with cyclohexane dehydrogenation via a Pd/Ag membrane. Unfortunately, none of these interesting systems have undergone experimental validation to date. Bradford et al. [44] studied the FT reaction in a contactor-type MR running in a “flow-through” mode (FTCMR) that used a catalytic porous alumina membrane. They observed a higher C2+ hydrocarbon yield and a lower

olefin/paraffin ratio in the MR than in the traditional reactor, and attributed the enhanced performance to be due to a higher H₂/CO-ratio prevailing within the catalytic membrane. Khassin and coworkers [45] also tested a similar concept and obtained high selectivity toward C5+ hydrocarbons, a higher space-time yield of liquid hydrocarbons, and up to three times higher catalyst activity with the FTCMR when compared with a slurry reactor.

In summary, the MR proposed to date for MeS use either Pd-type membranes for the controlled dosing of H₂ into the reactive mixture (these MR have yet to be tested experimentally, however) or MeOH/H₂O selective membranes in order to improve the MeS yield. The H₂O/MeOH-selective membranes that have been tested to date (Nafion®, silica) are unlikely to be robust long-term in the high-temperature and high-pressure MeS environment, however. And the robustness/performance of Pd membranes in the same conditions (temperatures <300 °C, in CO-rich environments at high pressures) remains to be validated experimentally (problems with applying such membranes in large-scale processes relating to the cost and/or availability of the metal, notwithstanding). In this work, we investigate, instead, a different process concept, in which a membrane with the desired characteristics serves as an interface contactor in between the MeS environment in the shell-side and a liquid sweep solvent flow in the membrane permeate-side. Tetraethylene glycol dimethyl ether (TGDE) is chosen as the solvent, because methanol has high solubility in it but permanent gases like H₂ and CO do not. TGDE also has a relative high boiling point (275 °C), which makes it robust to the MeS environment. By removing in situ the MeOH generated, this allows the reactor conversion to reach beyond equilibrium. In the proposed process, the separation selectivity is provided by the sweep liquid used and not the membrane, and thus commercial off-the-self inorganic membranes can be utilized, which require no further major developmental effort beyond modifying the hydrophobicity of their surface. One is, therefore, no longer constrained by the limited availability (or lack of robustness) of appropriate permselective membrane materials and can, instead, rely on a greater range of available liquid solvents to attain the desired selective properties. TGDE was also previously used by Westerterp et al. [46] in an absorptive trickle-bed MeS reactor. The potential advantages of using the proposed MR when compared to the trickle-bed reactor is that it provides (i) for better gas (G)-liquid (L) disengagement, (ii) for lower loss of solvent since in the latter reactor the solvent is in direct contact

with the catalyst, and in the MR (iii) the presence of the solvent does not interfere with catalyst function, since the syngas components do not have to diffuse through the liquid layer (coating the catalyst surface) to reach the catalyst.

2. Experimental Section

2.1 Experimental Set-Up

The schematic of the lab-scale experimental set-up is shown in Fig. 1. This set-up consists of three parts: the gas delivery system, the reactor module, and the gas analysis section. The inlet feed-stream is prepared by mixing the various gas components which are delivered from UHP gas cylinders, their flow rates being controlled via individual Mass Flow Controllers (MFC, Brooks 5400). The syngas mixture thus prepared is first pre-heated using heating tapes, and is then fed into the high-pressure and high-temperature MeS reactor. For the experiments reported here, the operating pressure range was 20-30 bar and the temperature range 200-240 °C. Three ceramic band-heaters, each controlled by an individual PID controller, were used to maintain the catalyst bed isothermal. A three-point thermocouple (from OMEGA) was inserted in the reactor to monitor the temperature at three different positions in the bed.

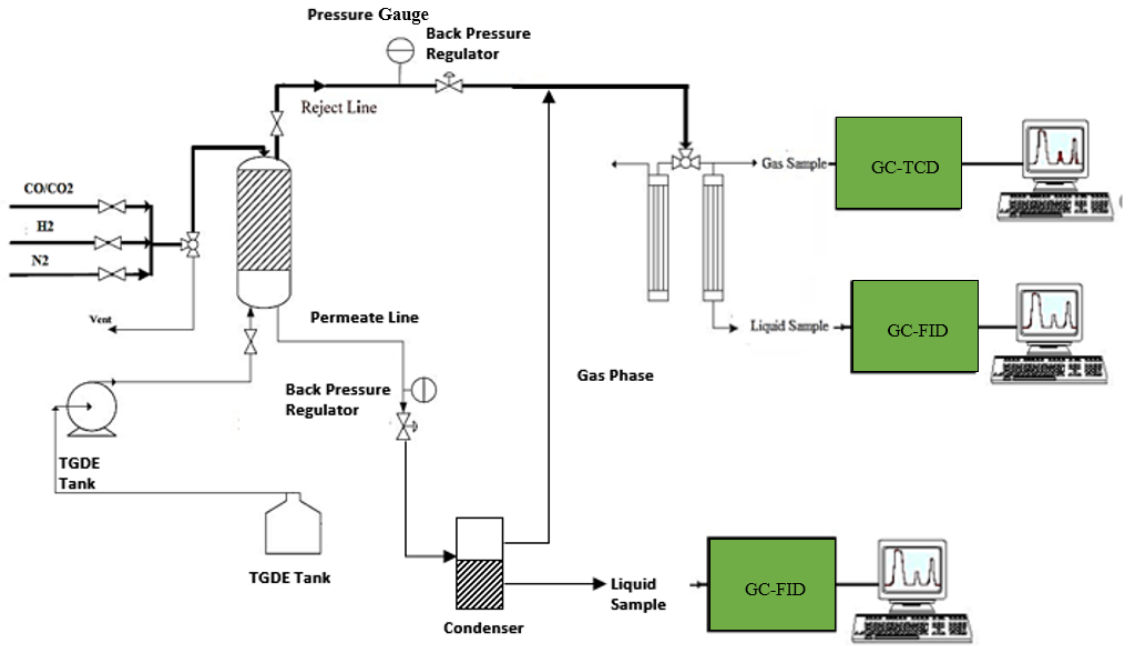


Figure 1 Schematic of the experimental set-up

A schematic of the membrane reactor itself is shown as Fig. 2. A tubular ceramic membrane (for further details, see discussion to follow) divides the reactor into two zones: the shell-side (often, also referred to as the reject-side) and the tube-side (permeate side). The catalyst is packed in the shell-side where the MeS reaction takes place, with the methanol that is produced transporting through the membrane and carried away by dissolving into the liquid sweep that flows through the tube-side. The pressure of the MR reject-side is controlled by a back-pressure regulator (BPR, TESCOM 26-1765-24-161). The gas stream exiting the BPR in the MR reject-side passes through a condenser, whose role is to condense the methanol, and potentially other liquid products of the MeS reaction for further analysis (to prevent any condensation on the tube walls, the tubing in between the reactor and the BPR is heated with heating tapes at 170 °C). The condenser is filled with glass beads (for more effective cooling of the gaseous stream) and is immersed in a cooling bath that contains a mixture of dry-ice and acetone, and whose temperature is maintained at -78 °C, thus ensuring the complete condensation of methanol and H₂O and any other potential MeS by-products in the gas outlet (however, the catalyst employed is highly selective, and in the experiments reported here only a minor amount of dimethyl ether (DME) has been observed). This

is verified by the fact that no MeOH or other organic compounds are detected in the gas stream (analyzed via a Gas Chromatograph equipped with a Thermal Conductivity Detector (GC-TCD, HP5890, column #Carboxe 1000) exiting the condenser that contains only CO, CO₂ and H₂. The composition of the liquid phase collected in the condenser is analyzed with a Gas Chromatograph equipped with a Flame Ionization Detector (GC-FID, HP5800, column # DB-1301).

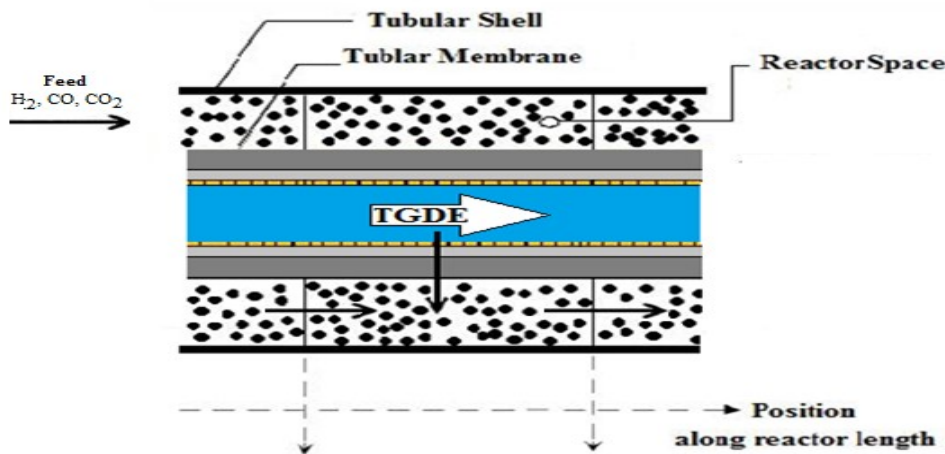


Figure 2. Schematic of the membrane reactor

The membrane permeate-side is connected to a liquid pumping system, that consists of the sweep liquid reservoir, a HPLC pump (and the associated tubing and valves), which is used to pump the sweep liquid through the tube-side of the membrane. The pressure of the membrane permeate-side is again controlled by a BPR (TESCOM 26-1765-24-161) installed in the exit line. After exiting the BPR, the liquid is depressurized into a condenser, that is installed after the BPR operating at room temperature and atmospheric pressure, in order to release any permanent gases (CO, CO₂ and H₂) that may potentially be dissolved in the sweep liquid. The gas stream from the liquid condenser is then re-combined with the gas stream exiting the MR shell-side BPR (for the purpose of properly closing mass balances), and the resulting total gas stream exiting the MR is sent to the reject-side condenser described above to collect the condensable vapors. The liquid-phase from the permeate-side condenser is analyzed with a GC-FID instrument. The same experimental set-

up is used for carrying out packed-bed reactor (PBR) experiments by closing both the inlet and exit of the permeate side of the membrane.

2.2 Experimental Procedure

In the experiments, a commercial Cu-based MeS catalyst (MK-121, from Haldor-Topsoe) was utilized, whose composition and other properties, as provided by the manufacturer, are shown in Table 1. Prior to loading into the reactor, the catalyst was ground, and 30 g of the powdered catalyst with particle sizes in the range from 650 μm to 850 μm were diluted with quartz of the same size, for the mixture to be loaded into the reactor. The reactor itself is an autoclave made of stainless steel, 4.2 cm in internal diameter (ID) and 21 cm in length.

Table 1. MK-121 catalyst properties, (catalyst cylinders with domed ends, 6x4 mm)

Property	Value
Chemical Composition	
Cu %	>43
Zn %	20 \pm 3
Al %	5 \pm 1
Graphite, Oxygen in the metallic oxides,	
Carbonates, moisture, %	Balance
Axial crush strength, kg/cm ²	>220
Expected filling density, kg/l	1

The membrane is attached to the top of the autoclave with flexible stainless steel tubing that allows for thermal expansion; it is connected to the tubing with the aid of Swagelok fittings and graphite gaskets. Before installing the membrane and loading the catalyst into the reactor, its bottom part is first filled with pure quartz particles with smaller sizes than the catalyst, in the range from 150 μm to 650 μm . Then, the membrane is installed with its bottom located just above the quartz particle bed, and the catalyst (intermixed with sufficient quantity of quartz to fill the reactor along

the length of the membrane) is added to create the MR section. Above the MR section, a bed of coarser quartz particles (size from 850 μm to 1000 μm) is then added. The feed into the reactor is through a tube that traverses the length of the reactor from the top of the autoclave in the middle of the fine quartz particle bed at the bottom of the reactor. When the reactor operates as a PBR, the inlet and outlet of the membrane permeate side are kept closed. The reactor operates isothermally, both in the PBR and the MR configurations, with the temperature difference across the whole reactor length being less than 2 $^{\circ}\text{C}$. The pressure drop in both reactor (PBR and MR) configurations is less than 0.1 bar.

Each experiment starts with the calibration of the various MFC's. Then, a leak test is performed, which involves pressurizing the reactor to 30 bar with N_2 , closing the reactor inlet and outlet, and monitoring the pressure. The reactor is considered “leak-free” and ready to initiate experiments with, if the pressure drop is determined to be <0.2 bar over a 24 h period (during the reactor experiments, the system sealing performance was also routinely monitored under flowing H_2 by monitoring and recording input and output flow rates). Then the catalyst activation step commences. The catalyst, as received from the manufacturer, is potentially in an oxidized state because of its prior exposure to atmospheric air conditions. Before beginning the experiments, the catalyst must, therefore, be activated via hydrogenation. For that, the reactor is heated to 180 $^{\circ}\text{C}$, at a rate of 50 $^{\circ}\text{C}/\text{h}$, in flowing N_2 (flow rate of 600 cc/min) at a pressure of 18 bar. In the next step, flowing H_2 is introduced into the reactor (12 vol.% in N_2), while keeping the total flow rate constant at 600 cc/min. Upon the introduction of H_2 , an initial increase (~ 10 $^{\circ}\text{C}$) in the temperature of the catalyst bed is observed (the hydrogenation reaction is exothermic), after which the temperature returns slowly back to its original value. After 3 h from the time the catalyst was first exposed to the H_2 mixture, the H_2 concentration is increased to 14 vol. %, and after waiting for 2 h, the same procedure (i.e., increments in concentration of 2 vol. %, waiting for 3 h, etc.) is repeated till the H_2 concentration reaches 18 vol. %. At that point, and after waiting for another 3 h, the catalyst bed temperature is increased to 200 $^{\circ}\text{C}$ at a rate of 10 $^{\circ}\text{C}/\text{h}$. In the next step, the hydrogen concentration is increased gradually to 22 vol.% over a period of 18 h while maintaining the total flow rate constant at 600 cc/min and the pressure at ~ 18 bar. When a H_2 concentration of 22 vol. % is reached, the reactor is left there for an additional 3 h in order to complete the activation process.

After the catalyst is activated, the reactor is purged with N₂ at a flow rate of 600 cc/min for ~ 1 h before starting the (PBR or MR) experiments. For each separate experiment, the experimental conditions are adjusted to the target values through the temperature controllers, the BPR's, the MFC's, the HPLC pump (for the MR experiments), etc. The reactor temperature and pressure are continuously monitored as is the outlet total gas flow rate (via bubble-flow meters) and composition (via GC-TCD). A steady state is assumed to be reached, when a constant outlet composition and flow is observed (less than 5% relative change in the concentration and less than 2% change in the outlet flow rate).

2.3 Membrane Preparation

We utilize in this project a multilayer ceramic membrane, from Media and Process Technology, Inc. (M&PT) whose properties, as reported by the manufacturer, are shown in Table 2. As explained above, the role of the membrane is to remove *in situ* the methanol that is generated in the shell-side while preventing the reactant gases from passing through. In order for the membrane to function that way, we maintain the pressure in the tube-side higher than that in the shell-side, so that the liquid will penetrate into the pores of the membrane, thus blocking the pathway for gas transport. We do not wish, however, the solvent to completely infiltrate the membrane because that may create a very large resistance for the MeOH molecules to permeate through (the desired configuration is shown schematically in Fig. 3). For that the membrane must be modified, so that its surface becomes hydrophobic to be able to prevent the solvent from completely penetrating through.

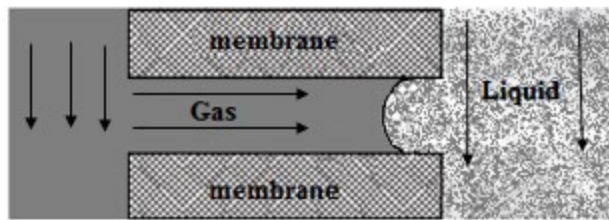


Figure 3. Gas-liquid phase contact in a hydrophobic membrane

Table 2. Properties of the ceramic membrane installed in the membrane reactor

Layer	Material	Thickness (μm)	Average pore size (\AA)
Support	α - Alumina	1100	2000- 4000
First layer	α - Alumina	10-20	500
Second layer	γ - Alumina	2-3	100
Outer Diameter (mm)		5.7	
Inner Diameter (mm)		4.7	

The M&PT ceramic membrane is intrinsically hydrophilic, so in order to modify its surface we have adapted a method first developed by Lu et al. [47], which uses a fluoroalkylsilane (FAS) compound with hydrolysable groups and hydrophobic ends [48] (see Fig. 4) as a surface modifier. It has been reported [47, 48] that FAS compounds attach to metal oxide surfaces through a reaction between their hydrolysable groups with the surface hydroxyl groups, as it is also shown schematically in Fig. 4. Prior to the modification step, the membrane is glazed on both ends, \sim 1 cm long, to ensure complete sealing when installed in the reactor. Further details about the glazing procedure are reported elsewhere [49].

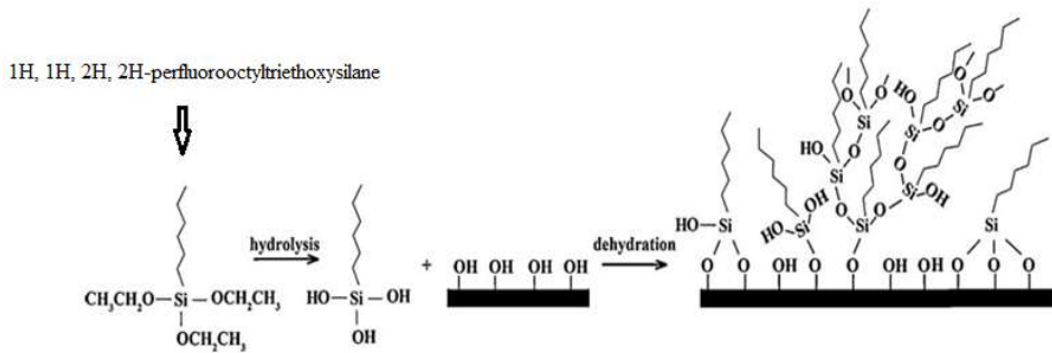


Figure 4. FAS attachment mechanism onto the membrane surface

For the surface modification, the membrane tube is cleaned via ultra-sonication, first in ethanol and then in de-ionized (DI) water for 30 min each. Then, the membrane is soaked in an ethanol/DI water solution (2:1 volume ratio) for 24 h, and then dried in air at 333 K for 24 h. The dry membrane is then immersed into a FAS/hexane (0.1 mol/l) solution (prepared by dissolving FAS into hexane under vigorous stirring for 12 h at room temperature), ultra-sonicated for 30 min and then left in the FAS solution for an additional 24 h to allow the surface coupling reaction to complete. The membrane is then rinsed multiple times with hexane to remove any unreacted FAS from its surface and is then dried in an oven at 373 K for 12 h. The membrane soaking in the FAS/hexane, washing and drying steps are then repeated 4 times, and the modified membrane is then placed in a furnace and heated in flowing Ar at 200 °C for 6 h.

After the modification, the membrane surface becomes visibly hydrophobic (see Fig 5 showing DI water droplets placed on the membrane tube). To more quantitatively assess the ability of the modification procedure to render the membrane surface hydrophobic and to establish the detailed procedure, a number of characterization tests are carried out. They include break-through pressure tests, contact angle measurements, membrane morphology testing via electron microscopy (SEM), FTIR-DRIFTS characterization (to verify that the surface coupling reaction has, indeed, taken place), and thermogravimetric analysis (TGA) to verify that the surface modification is robust at the temperatures employed in MeS. The results of these studies are reported in greater detail elsewhere [50].

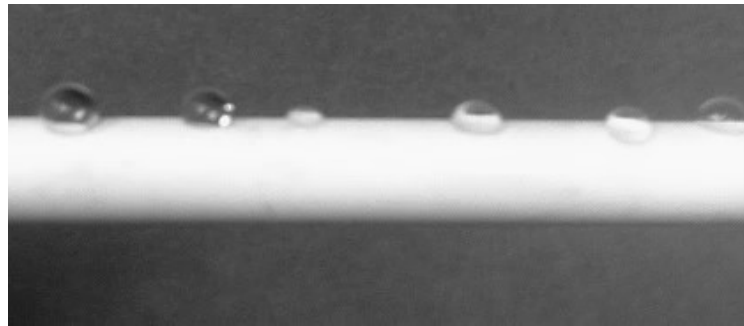


Figure 5. DI water drops on the surface of the modified membrane

Prior to the initiation of the MR experiments, the ability of the modified membrane to prevent complete infiltration (and thus break-through) of the solvent employed as a sweep (TGDE in this study) is tested at room temperature. For that, the solvent is allowed to flow through the membrane tube-side at a pressure which is ~1.5 bar higher than the membrane shell-side, which is kept at 1 bar under flowing N₂. The solvent exiting the membrane is recycled continuously back into its reservoir and from there back into the membrane tube-side. The leak rate is then estimated from the change in the mass of solvent in the reservoir after a certain time period. The membrane surface modification and the membrane sealing are considered successful, and the MR experiment is initiated, if the rate of solvent loss is smaller than 2 ml/day.

Despite efforts to tightly seal the membrane and to appropriately modify the membrane surface, some solvent loss is unavoidable during the extended membrane reactor experimental runs. To prevent the solvent that may have infiltrated through from potentially interfering with the reactor runs (e.g., deactivating the catalyst), at regular intervals (typically after ~16 h of continuous MR operation) the reactor experiment is interrupted to rid the MR of any solvent that may have accumulated (physically adsorbed) on the surface of the catalyst. For that, the solvent flow is first stopped, and the reactor feed is replaced with a pure H₂ flow (150 cc/min) at 220 °C. After flushing the reactor at these conditions for ~1 h, the reactor pressure is lowered to atmospheric and the system is left under H₂ flow at 220 °C overnight to purge any infiltrated solvent out of the reactor.

(It should be noted, however, that in fact we have no evidence from our lab-scale study that catalyst deactivation is caused by solvent accumulation, but out of over-abundance of caution we still followed the aforementioned catalyst regeneration protocol through the whole MR/PBR study. We do find no mention of catalyst deactivation in the Westerterp et al. study [46] either).

3. Results and Discussion

Prior to the initiation of the MR experiments, a series of experiments were performed with the membrane permeate-side inlet and outlet being closed and the system operating as a PBR. The purpose of these experiments was two-fold: First, to provide the basis for comparison for the MR experiments, i.e., whether the MR performs better or worse than the PBR under identical experimental conditions; and second to generate the experimental data needed to fit a global rate expression from the technical literature to be employed in a MR model to be subsequently used for further process design and scale-up (the development of such a model goes beyond the scope of this experimental paper, however, and will be described in a future publication [51]). In the PBR experiments, we study the impact on the performance of the reactor of five key parameters, namely temperature (T), pressure (P), catalyst weight to inlet molar flow-rate ratio (W/F), the carbon factor in the feed ($CF = \text{mol CO} / (\text{mol CO} + \text{mol CO}_2)$), and the feed stoichiometric number ($SN = (\text{mol H}_2 - \text{mol CO}_2) / (\text{mol CO} + \text{mol CO}_2)$). Our experiments indicate that the MeOH selectivity is always higher than 98 %, so global rate expressions for reactions R1 and R3 developed by Vanden Bussche et al. [52] (based on a prior mechanism for R3 by Rozovskii and Lin [53] and Chinchen et al. [54]) and thermodynamic parameters from Graaf et al. [55] were tested to verify whether they are in agreement with the experimental data.

Fig. 6 shows an iso-conversion graph plotting the predicted (by fitting the global reaction rate expressions of Vanden Bussche et al. [52]) carbon conversion (defined by Eqn. 1 below) values vs. the experimental data, indicating a good agreement between model and experiments. (further details about the methods employed for parameter fitting, and the use of the derived global rate expressions in the MR model for design and scale-up will be presented elsewhere [51]).

$$X_{carbon} = \frac{(F_{inlet\ CO} + F_{inlet\ CO_2}) - (F_{outlet\ CO} + F_{outlet\ CO_2})}{(F_{inlet\ CO} + F_{inlet\ CO_2})} * 100 \quad (1)$$

where F_i is the molar flow rate (mol/s) of species i at the designated location.

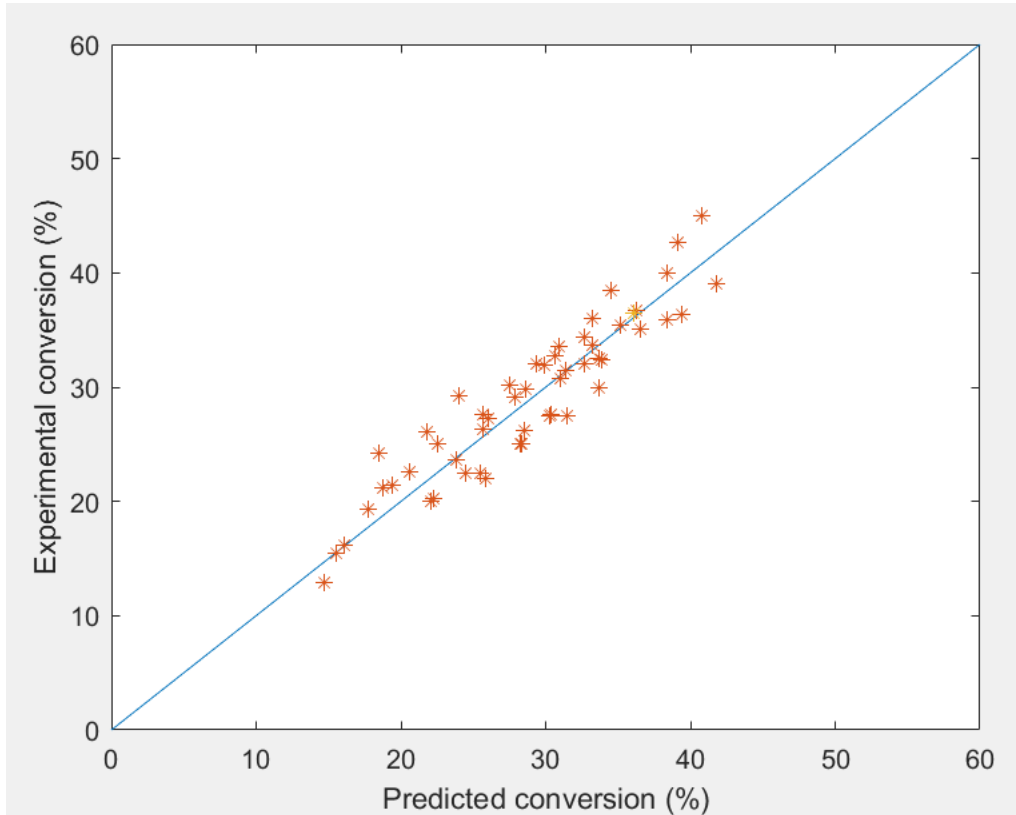


Figure 6. Iso-conversion plot of experimental vs. predicted carbon conversions

In the membrane reactor experiments, in order to prevent the solvent from completely wetting the membrane, its surface is rendered hydrophobic, as noted in Sec. 2.3. To prevent the gases in the reaction side (membrane shell-side) from **bubbling-through** into the membrane tube-side, the pressure of the latter is maintained ~ 1 bar higher than that of the reaction side. By employing a liquid sweep in the tube-side, the methanol generated in the shell-side is removed in situ from the reactor side, resulting in a shift of equilibrium toward methanol. (In a commercial setting, the methanol would then be removed from the resulting TGDE/MeOH stream, with the solvent being recycled back into the MR – in the experiments reported here fresh, pure TGDE

solvent is used for the duration of each run). One other key role of the solvent sweep, from a process design standpoint, is for carrying away the exothermic heat of reaction. The membrane plays an important role in the process as an interphase contactor between the reactive mixture and the product removing solvent, without requiring the solvent to come directly in contact with the catalyst (as is the case with employing trickle-bed reactors), thus reducing the impact that the catalyst may have on solvent stability and vice versa, and as a result prolonging their life-times.

A series of experiments are reported here aiming to investigate the performance of the membrane reactor under different temperatures, pressures, sweep liquid flow rates, and W/F (catalyst weight/total molar flow rate), and to compare its behavior with that of the PBR under the same conditions. For these initial series of experiments, we have kept constant both the stoichiometric number ($SN = 1.96$) as well as the carbon factor ($F_{CO}/(F_{CO} + F_{CO_2}) = 0.625$)

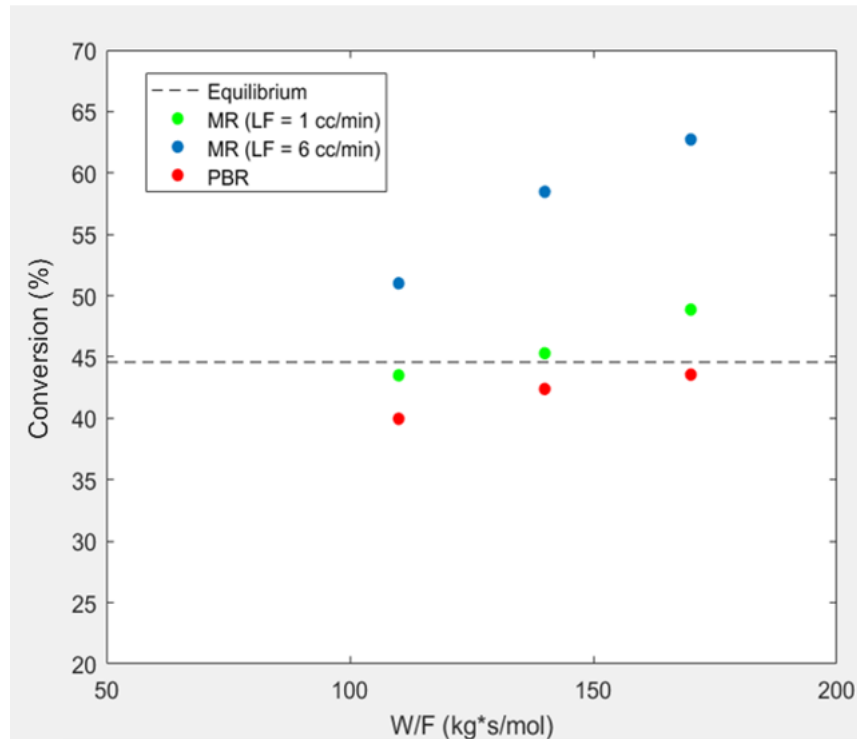


Figure 7. Effect of W/F on MR and PBR conversion. $P = 32$ bar, $T = 220$ °C

Fig. 7 plots the MR conversion vs. W/F for a shell-side (reactor-side) pressure of 32 bar, a temperature of 220 °C, and two different sweep liquid flow rates (LF). Shown on the same figure

are the corresponding PBR conversions as well as the calculated equilibrium conversion. As expected, both the MR and the PBR conversions increase with increasing W/F (in our case this is equivalent to decreasing the syngas flow rate since the catalyst weight and the syngas composition are kept constant in these experiments). Note that the conversion for the PBR, though increasing with W/F, still remains below the equilibrium conversion, which for these conditions, despite the relatively low temperature employed, is still fairly low (~44%). For the MR runs, employing the low sweep liquid flow rate (LF=1 cc/min), the MR conversion begins below the equilibrium line, but crosses the line as the W/F increases, and eventually exceeds the equilibrium. For the MR runs employing the higher sweep flow rate (LF=6 cc/min), the MR conversion exceeds the corresponding equilibrium conversion for all W/F values studied, being higher by ~ 50% for the highest W/F value studied.

To further explore the effect of sweep liquid, a series of experiments were carried out at a shell-side MR pressure of 32 bar, a temperature of 220 °C, and at a fixed value of W/F= 170 kg*s/mol while varying the sweep liquid flow rate, and the results are shown in Fig. 8, which shows the effect of increasing the sweep liquid flow rate on the MR conversion. As expected, the reactor conversion increases with increasing liquid sweep flow rates, with all MR conversions under these conditions exceeding the thermodynamic values (it should be noted, that in the experiments reported in Fig. 8 and throughout this paper, in order to maintain reactor isothermality, the liquid sweep was preheated to the operating temperature prior to entering the membrane tube-side). This is because a higher liquid sweep flow rate helps to remove a larger amount of methanol from the reaction side, and in so doing pushes further the equilibrium toward methanol generation. There is, of course, a limit of how high of a flow rate one can employ, since the higher the flow rate is the more dilute the MeOH concentration will be, which then negatively impacts downstream processing. Selecting the most optimal liquid sweep flow rate is, therefore, an important aspect of process optimization, which goes beyond the scope of the present paper, however, and will be dealt with in a forthcoming paper [51].

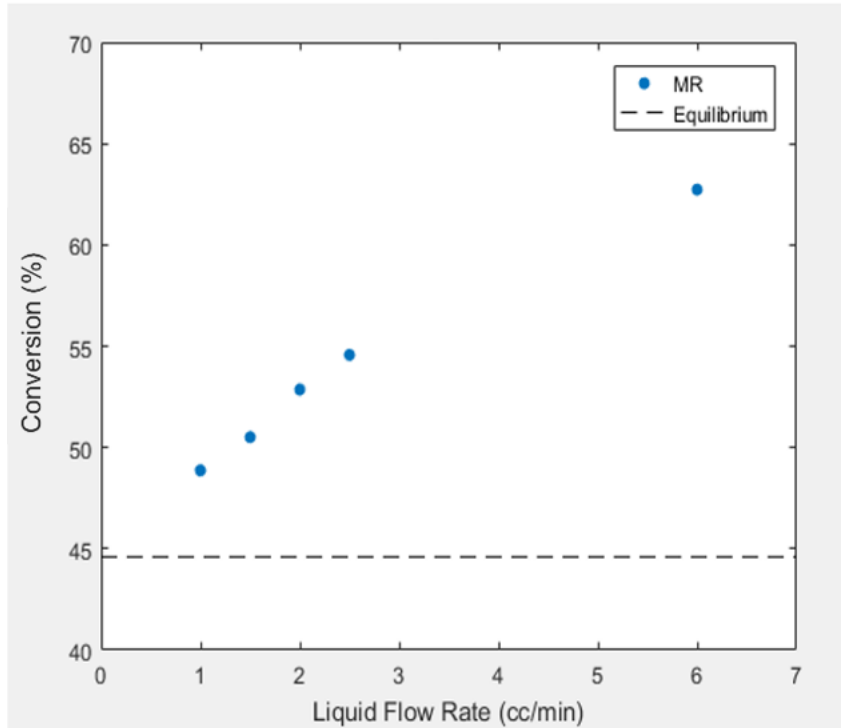


Figure 8. Effect of liquid sweep flow rate on MR conversion. $P = 32$ bar, $T = 220$ $^{\circ}\text{C}$, $\text{W/F} = 170$

$\text{kg}^*\text{s/mol}$

Fig. 9 shows a series of experiments in which the MR shell-side pressure was set at 32 bar, the sweep liquid flow rate was set at 1 cc/min, and W/F was set equal to 170 $\text{kg}^*\text{s/mol}$, and the reactor temperature was varied. The figure compares the experimental MR conversions with the conversion in a PBR under the same experimental conditions. The fairly narrow range of temperatures studied is due to concerns about damaging the FAS coating that renders the membrane surface hydrophobic (because with this particular silylating agent a safe operating temperature is < 230 $^{\circ}\text{C}$ [50]) and because of concerns with catalyst selectivity (the catalyst manufacturer recommends a reaction temperature higher than 190 $^{\circ}\text{C}$ in order to prevent the production of wax). As shown in the figure, the conversion of MR increases with increasing temperature, due likely to the increased reaction rate and methanol transport across the membrane as the temperature increases. However, for the PBR, the conversion passes through a maximum with the reactor conversion at $T = 220$ $^{\circ}\text{C}$ being lower than that at $T = 214$ $^{\circ}\text{C}$, due likely to thermodynamic limitations coming into play under this relatively high W/F and temperature

conditions. Shown on the same figure are the calculated equilibrium conversions. Note, that at this low temperature, the equilibrium conversion is high but the PBR conversion is low because of the low reaction rate prevailing at these conditions. At the temperature of 220 °C, the PBR conversion approaches the equilibrium conversion and under this condition, the membrane reactor attains a conversion that is higher than the PBR conversion but also the equilibrium conversion as well. For all the experiments presented here, the MR conversions are higher than the corresponding PBR values, though the gains are relatively modest due to the size of the membrane utilized, and the low value of liquid sweep flow rate employed.

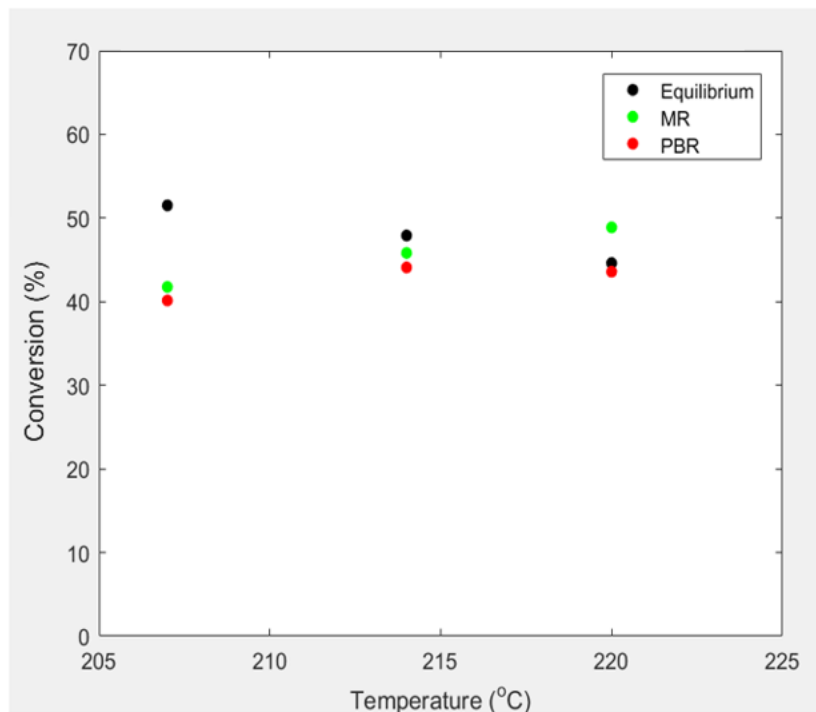


Figure 9. Effect of temperature on PBR, MR and equilibrium conversion. $P = 32$ bar, liquid sweep rate = 1 cc/min, $W/F = 170$ kg*s/mol.

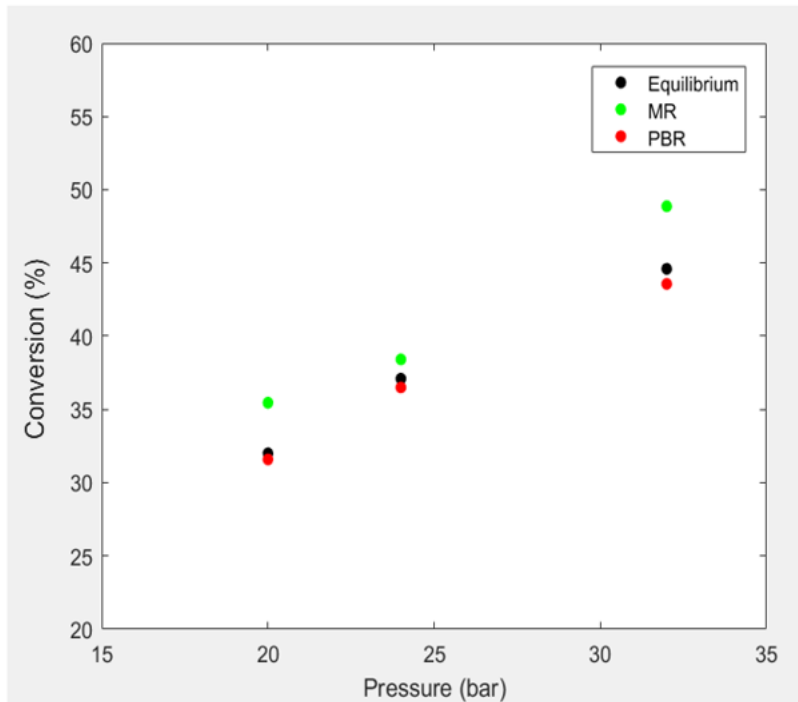


Figure 10. Effect of pressure on PBR, MR and equilibrium conversion. $T = 220\text{ }^{\circ}\text{C}$, liquid sweep rate = 1 cc/min, $\text{W/F} = 170\text{ kg}^*\text{s/mol}$

Finally, Fig. 10 shows a series of experiments in which the MR temperature was set at 220 $^{\circ}\text{C}$, the sweep liquid flow rate was set at 1 cc/min, and W/F was set equal to 170 $\text{kg}^*\text{s/mol}$, and the MR shell-side pressure was varied. The figure again compares the experimental MR conversions with the conversion in a PBR under the same experimental conditions; shown on the same figure are also the calculated equilibrium conversions. As one can see, at this relatively high temperature the BPR conversions are fairly close to the equilibrium conversions, particularly for the lower pressures. For all conditions in this figure, the MR exhibits conversions that are higher than equilibrium. The MR, PBR and the calculated equilibrium conversions all increase with increasing pressure, which is to be expected since the MeS reaction results in an overall reduction in the number of moles and is, thus, thermodynamically favored at higher pressures. An added reason for the increase in the MR conversion with increasing pressure, in addition to more methanol being generated, is that the increase in pressure means that a higher amount of methanol transports through the membrane and is removed by the TGDE, thus further shifting the equilibrium towards

the methanol generation side. For the whole range of pressures studied, the MR attains higher conversions than the PBR.

Though limitations with the lab-scale experimental system, which only accommodates one membrane, prevents us from investigating a wider range of experimental conditions, the aforementioned data-validated MR model allows one to access a much broader range of conditions for process scale-up and design purposes in order to study the practical feasibility of the proposed technology. The model predicts, for example, in line with experimental observations, that an increase in reactor pressure and space time (i.e., W/F) are both beneficial for the performance of the MR. For sufficiently high pressures, membrane area and W/F values, the model indicates that conversions close to 90 % are attained in the MR, significantly higher than the equilibrium conversions under these conditions. Preliminary economic evaluations indicate that such high conversions (~85%) would allow the proposed process to operate on biomass-derived syngas in one-pass configuration without recycle of unreacted syngas needed. Further discussions describing the basic physics of the model and the assumptions, and detailed presentation of the model results and predictions will be presented in a future publication [51].

4. Conclusions

In this paper, a novel liquid sweep membrane reactor has been studied experimentally. In the reactor, we employ commercial mesoporous alumina membranes whose surface is rendered hydrophobic via the application of a fluorosurfactant agent. A high B.P. liquid with good solubility toward methanol flows in the tube-side of the membrane to remove *in situ* the methanol from the reaction zone, thus helping the MR to attain conversions higher than the thermodynamic equilibrium conversions and those observed in a PBR under similar experimental conditions. Though due to the limited size of membrane as well as of the reactor itself, the reported gains in conversion are generally modest, preliminary process scale-up simulations employing a data-validated model indicate the potential of the proposed concept to attain per single-pass conversions greater than 85%, which will make the proposed MR system applicable for distributed-type biomass gasification applications.

The proposed MR design shares the same conceptual basis with the absorptive gas-liquid-solid (GLS) trickle-bed reactor [46], since both reactive separation technologies in their application to MeS employ a high B.P. solvent to in situ remove the MeOH, and thus favorably shift the reactor conversion and yield. We believe, however, that the present MeS MR system has a number of potential advantages over the absorptive reactor system. They include (i) better G-L disengagement, (ii) less solvent volatilization, and most importantly (iii) less reactive loss of solvent (and potentially catalyst deactivation).

For the application of the technology we envision (i.e., alcohol synthesis in the context of distributed-type biomass gasification applications), the key advantage of both reactive separation MeS technologies is to attain high conversions to the level where no syngas recycle will be needed. A second advantage is to use the liquid sweep to remove some of the reaction's exothermic heat. A potential disadvantage for both processes, compared to the conventional fixed-bed reactor MeS technology, is the fact that a portion of the alcohol ends-up in the solvent, from which alcohol needs to be separated out via distillation. Though we have not, as yet, completed a technical and economic analysis (TEA) for the process, we do not expect this to be a particularly challenging separation, however, given the differences in the boiling point between the two compounds

Our studies of the MeS MR process are continuing, with a key focus being process optimization and scale-up. A key optimization condition, for example, is the concentration of the alcohol in the solvent, since it correlates with reactor conversion and, of course, with product separation and recovery. It depends in a complex way on catalyst weight (and its activity), the membrane area utilized (and its transport characteristics), the solvent flow and the rest of the experimental parameters (e.g., temperature, pressure, syngas composition). Another related key optimization condition is the fraction of the alcohol product recovered in the product stream. In the experiments reported here, it varied from ~75% to more than 90%, but it also depends in a complex way on catalyst weight and activity, membrane area and permeation characteristics, the solvent flow and the rest of the experimental parameters. We employ in our process design and optimization studies the data-validated MR model, since it allows us to access a significantly broader range of operating conditions than it is otherwise possible with the present lab-scale

experimental set-up. Key findings and conclusions from such optimization and scale-up will be presented in an upcoming publication [51].

A key future Task in our ongoing studies of the MR-based high-pressure alcohol synthesis process is to further validate the potential advantages noted for the MR technology over its sister reactive separation absorptive technology in side-by-side comparisons with similar catalysts, solvents, syngas compositions and other experimental conditions. In particular, a key emphasis will be to compare the G-L transport characteristics for the two configurations in side-by-side modeling and experiments.

Acknowledgement

The support of the National Science Foundation (Award# CBET-1705180) is gratefully acknowledged. Many helpful interactions and discussions with Dr. Sahar Soltani and Dr. Nazanin Entesari are also gratefully acknowledged.

References

- [1] C. Pieper, H. Rubel, Electricity storage: Making large-scale adoption of wind and solar energies a reality, *Balanced Growth*, Springer, 2012, pp. 163-181.
- [2] A. Behr. Methanol: The Basic Chemical and Energy Feedstock of the Future. Asinger's Vision Today. Edited by Martin Bertau, Heribert Offermanns, Ludolf Plass, Friedrich Schmidt and Hans-Jürgen Wernicke. *Angewandte Chemie International Edition*, 53 (2014) 12674.
- [3] E. Unneberg, S. Kolboe, Formation of p-Xylene from Methanol over H-ZSM-5, *Studies in Surface Science and Catalysis*, Elsevier, 1988, pp. 195-199.
- [4] M. Conte, J.A. Lopez-Sanchez, Q. He, D.J. Morgan, Y. Ryabenkova, J.K. Bartley, Modified zeolite ZSM-5 for the methanol to aromatics reaction. *Cat. Sci. & Technol.*, 2 (2012) 105-112.
- [5] D. Zeng, J. Yang, J. Wang, J. Xu, Y. Yang, C. Ye, Solid-state NMR studies of methanol-to-aromatics reaction over silver exchanged HZSM-5 zeolite. *Microporous and Mesoporous Materials*, 98 (2007) 214-219.

[6] B. Elvers. *Handbook of Fuels*. Wiley-VCH, Wiesbaden, 2008.

[7] CMAI. *World Methanol Analysis*.
<https://www.chemicalonline.com/doc/cmai-completes-2010-world-methanol-analysis-0001>
accessed 2010.

[8] CMAI. *World Butylenes Analysis*.
<https://ihsmarkit.com/industry/chemical.html> (accessed 2010).

[9] W.T. Hess, A. Kurtz, and D. Stanton. *Kirk-Othmer Encyclopedia of Chemical Technology*. 1995.

[10] K. Aasberg-Petersen, C.S. Nielsen, I. Dybkjær, and J. Perregaard. Large scale methanol production from natural gas. *Haldor Topsoe*, 22 (2008).

[11] Q. Zhang, D. He, and Q. Zhu. Recent progress in direct partial oxidation of methane to methanol. *J. Nat. Gas Chem.*, 12 (2003) 81-89.

[12] T. Choudhary, D. Goodman. Methane decomposition: production of hydrogen and carbon filaments. *Catalysis*, 19 (2006) 164-183.

[13] H.F. Abbas, W.W. Daud. Hydrogen production by methane decomposition: a review. *Int. J. Hydrogen Energy*, 35 (2010) 1160-1190.

[14] N. Muradov. Hydrogen via methane decomposition: an application for decarbonization of fossil fuels. *Int. J. Hydrogen Energy*, 26 (2001) 1165-1175.

[15] N. Muradov, T. Veziroğlu. From hydrocarbon to hydrogen–carbon to hydrogen economy. *Int. J. Hydrogen Energy*, 30 (2005) 225-237.

[16] M. Merkx, D.A. Kopp, M.H. Sazinsky, J.L. Blazyk, J. Müller, and S.J. Lippard. Aktivierung von Disauerstoff und Hydroxylierung von Methan durch lösliche Methan-Monooxygenase: eine Geschichte von zwei Eisenatomen und drei Proteinen. *Angewandte Chemie*, 113 (2001) 2860-2888.

[17] S.I. Chan, Y. Lu, P. Nagababu, S. Maji, M. Hung, M.M. Lee, I.J. Hsu, P.D. Minh, J.C. Lai, K.Y. Ng, S. Ramalingam. Efficient oxidation of methane to methanol by dioxygen mediated by tricopper clusters. *Angewandte Chemie International Edition*, 52 (2013) 3731-3735.

[18] R. Espinoza, E. Du Toit, J. Santamaria, M. Menendez, J. Coronas, S. Irusta, Use of membranes in Fischer-Tropsch reactors, *Studies in Surface Science and Catalysis*, Elsevier, 2000, pp. 389-394.

[19] S. Soltani, M. Sahimi, and T. Tsotsis. Catalytic membrane reactors. Encyclopedia of Membrane Science and Technology, (2013).

[20] F. Gallucci, L. Paturzo, and A. Basile. An experimental study of CO₂ hydrogenation into methanol involving a zeolite membrane reactor. *Chem. Eng. Proc.: Proc. Intens.*, 43 (2004) 1029-1036.

[21] G. Barbieri, G. Marigliano, G. Golemme, and E. Drioli. Simulation of CO₂ hydrogenation with CH₃OH removal in a zeolite membrane reactor. *Chem. Eng. J.*, 85 (2002) 53-59.

[22] M. Rahimpour, S. Ghader. Theoretical investigation of a Pd-membrane reactor for Methanol synthesis. *Chem. Eng. Technol.*, 26 (2003) 902-907.

[23] Struis, Rudolf Paul Wilhelm Jozef, S. Stucki, M. Wiedorn. A membrane reactor for methanol synthesis. *J. Membr. Sci.*, 113 (1996) 93-100.

[24] R. Struis, S. Stucki. Verification of the membrane reactor concept for the methanol synthesis. *Appl. Catal. A: General*, 216 (2001) 117-129.

[25] G. Chen, Q. Yuan. Methanol synthesis from CO₂ using a silicone rubber/ceramic composite membrane reactor. *Sep. Pur. Technol.*, 34 (2004) 227-237.

[26] M.P. Rohde, D. Unruh, G. Schaub. Membrane application in Fischer–Tropsch synthesis reactors - Overview of concepts. *Catal. Today*, 106 (2005) 143-148.

[27] M.P. Rohde, D. Unruh, G. Schaub. Membrane application in Fischer– Tropsch synthesis to enhance CO₂ hydrogenation. *Ind. Eng. Chem. Res*, 44 (2005) 9653-9658.

[28] M. Farsi, A. Jahanmiri. Dynamic modeling of a H₂O-permselective membrane reactor to enhance methanol synthesis from syngas considering catalyst deactivation. *J. Nat. Gas Chem.*, 21 (2012) 407-414.

[29] S.T. Leonard, S. Miachon, D. Vanhove. Effet de la nature de la membrane sur la synthese de Fischer-Tropsch en reacteur catalytique membranaire a lit fixe. *Recents Progres en Genie des Procedes*. 89 (2003) 226-231.

[30] S.L. D. Vanhove. Synthese de Fischer-Tropsch en alimentations separees (IMPBR). *Recents Progres en Genie des Procedes*. 89 (2003) 194–198.

[31] M. Rahimpour, A. Mirvakili, and K. Paymooni. A novel water perm-selective membrane dual-type reactor concept for Fischer–Tropsch synthesis of GTL (gas to liquid) technology. *Energy*, 36 (2011) 1223-1235.

[32] A. Forghani, H. Elekai, and M. Rahimpour. Enhancement of gasoline production in a novel hydrogen-permselective membrane reactor in Fischer–Tropsch synthesis of GTL technology. *Int. J. Hydrogen Energy*, 34 (2009) 3965-3976.

[33] M.A. Marvast, M. Sohrabi, S. Zarrinpashne, G. Baghmisheh. Fischer-Tropsch synthesis: Modeling and performance study for Fe-HZSM5 bifunctional catalyst. *Chem. Eng. Technol.*, 28 (2005) 78-86.

[34] R. Vakili, M. Rahimpour, R. Eslamloueyan. Incorporating differential evolution (DE) optimization strategy to boost hydrogen and DME production rate through a membrane assisted single-step DME heat exchanger reactor. *J. Nat. Gas Sci. Eng.*, 9 (2012) 28-38.

[35] M. Rahimpour, M. Dehnavi, F. Allahgholipour, D. Iranshahi, S. Jokar. Assessment and comparison of different catalytic coupling exothermic and endothermic reactions: a review. *Appl. Energy*, 99 (2012) 496-512.

[36] M. Bayat, M. Rahimpour. Simultaneous hydrogen injection and in-situ H₂O removal in a novel thermally coupled two-membrane reactor concept for Fischer–Tropsch synthesis in GTL technology. *J. Nat. Gas Sci. Eng.*, 9 (2012) 73-85.

[37] M. Bayat, M. Rahimpour. Simultaneous hydrogen and methanol enhancement through a recuperative two-zone thermally coupled membrane reactor. *Energy Systems*, 3 (2012) 401-420.

[38] M. Bayat, M. Rahimpour, M. Taheri, M. Pashaei, S. Sharifzadeh. A comparative study of two different configurations for exothermic–endothermic heat exchanger reactor. *Chem. Eng. Proc.: Proc. Intens.*, 52 (2012) 63-73.

[39] M. Bayat, M. Rahimpour. Simultaneous utilization of two different membranes for intensification of ultrapure hydrogen production from recuperative coupling autothermal multitubular reactor. *Int. J. Hydrogen Energy*, 36 (2011) 7310-7325.

[40] M. Rahimpour, M. Bayat. Production of ultrapure hydrogen via utilizing fluidization concept from coupling of methanol and benzene synthesis in a hydrogen-permselective membrane reactor. *Int. J. Hydrogen Energy*, 36 (2011) 6616-6627.

[41] M. Khademi, M. Rahimpour, A. Jahanmiri. Differential evolution (DE) strategy for optimization of hydrogen production, cyclohexane dehydrogenation and methanol synthesis in a hydrogen-permselective membrane thermally coupled reactor. *Int. J. Hydrogen Energy*, 35 (2010) 1936-1950.

[42] M. Khademi, P. Setoodeh, M. Rahimpour, A. Jahanmiri. Optimization of methanol synthesis and cyclohexane dehydrogenation in a thermally coupled reactor using differential evolution (DE) method. *Int. J. Hydrogen Energy*, 34 (2009) 6930-6944.

[43] M. Khademi, M. Rahimpour, and A. Jahanmiri. A comparison of a novel recuperative configuration and conventional methanol synthesis reactor. *Chem. Eng. Commun.*, 199 (2012) 889-911.

[44] C.J. M. Bradford, M. Te., A. Pollack. Monolith loop catalytic membrane reactor for Fischer–Tropsch synthesis. *Appl Catal A: Gen.* 283 (2005) 39–46.

[45] A. Khassin, A. Sipatrov, T. Yurieva, G. Chermashentseva, N. Rudina, V. Parmon. Performance of a catalytic membrane reactor for the Fischer–Tropsch synthesis. *Cat. Today*, 105 (2005) 362-366.

[46] K.R. Westerterp, M. Kuczynski, T.N. Bodewes, M.S. Vrijland. Neue Konvertersysteme für die Methanol-Synthese. *Chem. Ing. Technik*, 61 (1989) 193-199.

[47] J. Lu, Y. Yu, J. Zhou, L. Song, X. Hu, A. Larbot. FAS grafted superhydrophobic ceramic membrane. *Appl. Surf. Sci.*, 255 (2009) 9092-9099.

[48] C.C. Wei, K. Li. Preparation and characterization of a robust and hydrophobic ceramic membrane via an improved surface grafting technique. *Ind. Eng. Chem. Res.*, 48 (2009) 3446-3452.

[49] Z. Li. Methanol Synthesis in a Contactor-Type Membrane Reactor, PhD Thesis USC. (2017).

[50] S. Soltani. Methanol Synthesis in a Membrane Reactor, PhD Thesis USC. (2014).

[51] Z. Li, T.T. Tsotsis. Modeling and simulation study of methanol synthesis in a high-pressure membrane reactor, Paper in Preparation.

[52] K.V. Vanden Bussche, G. Froment. A Steady-State Kinetic Model for Methanol Synthesis and the Water Gas Shift Reaction on a Commercial Cu/ZnO/Al₂O₃ Catalyst. *J. Catal.*, 161 (1996) 1-10.

[53] A.Y. Rozovskii, G.I. Lin. Fundamentals of methanol synthesis and decomposition. *Topics in Catalysis*, 22 (2003) 137-150.

[54] G. Chinchen, P. Denny, D. Parker, M. Spencer, D. Whan. Mechanism of methanol synthesis from CO₂/CO/H₂ mixtures over copper/zinc oxide/alumina catalysts: use of ¹⁴C-labelled reactants. *Appl. Catal.*, 30 (1987) 333-338.

[55] G. Graaf, E. Stadhuis, A. Beenackers. Kinetics of low-pressure methanol synthesis. *Chem. Eng. Sci.*, 43 (1988) 3185-3195.